Cage-like Copper(II) Silsesquioxanes: Transmetalation Reactions and Structural, Quantum Chemical, and Catalytic Studies

Alexey Bilyachenko, Marina Dronova, Alexey yalymov, Frédéric Lamaty, Xavier Bantreil, Jean Martinez, Christelle Bizet, Lidia Shul'Pina, Alexander Korlyukov, Dmitry Arkhipov, et al.

▶ To cite this version:

HAL Id: hal-03079243
https://hal.archives-ouvertes.fr/hal-03079243

Submitted on 1 Mar 2021

Cage-like Copper(II) Silsesquioxanes: Transmetalation Reactions and Structural, Quantum Chemical, and Catalytic Studies

Alexey N. Bilyachenko,*[a] Marina S. Dronova,[a] Alexey I. Yalymov,[a] Frédéric Lamaty,*[b] Xavier Bantreil,[b] Jean Martinez,[b] Christelle Bizet,[b] Lidia S. Shul'pina,[a] Alexander A. Korlyukov,*[a, c] Dmitry E. Arkhipov,[a] Mikhail M. Levitsky,*[a] Elena S. Shubina,[a] Alexander M. Kirillov,[d] and Georgiy B. Shul'pin*[e]
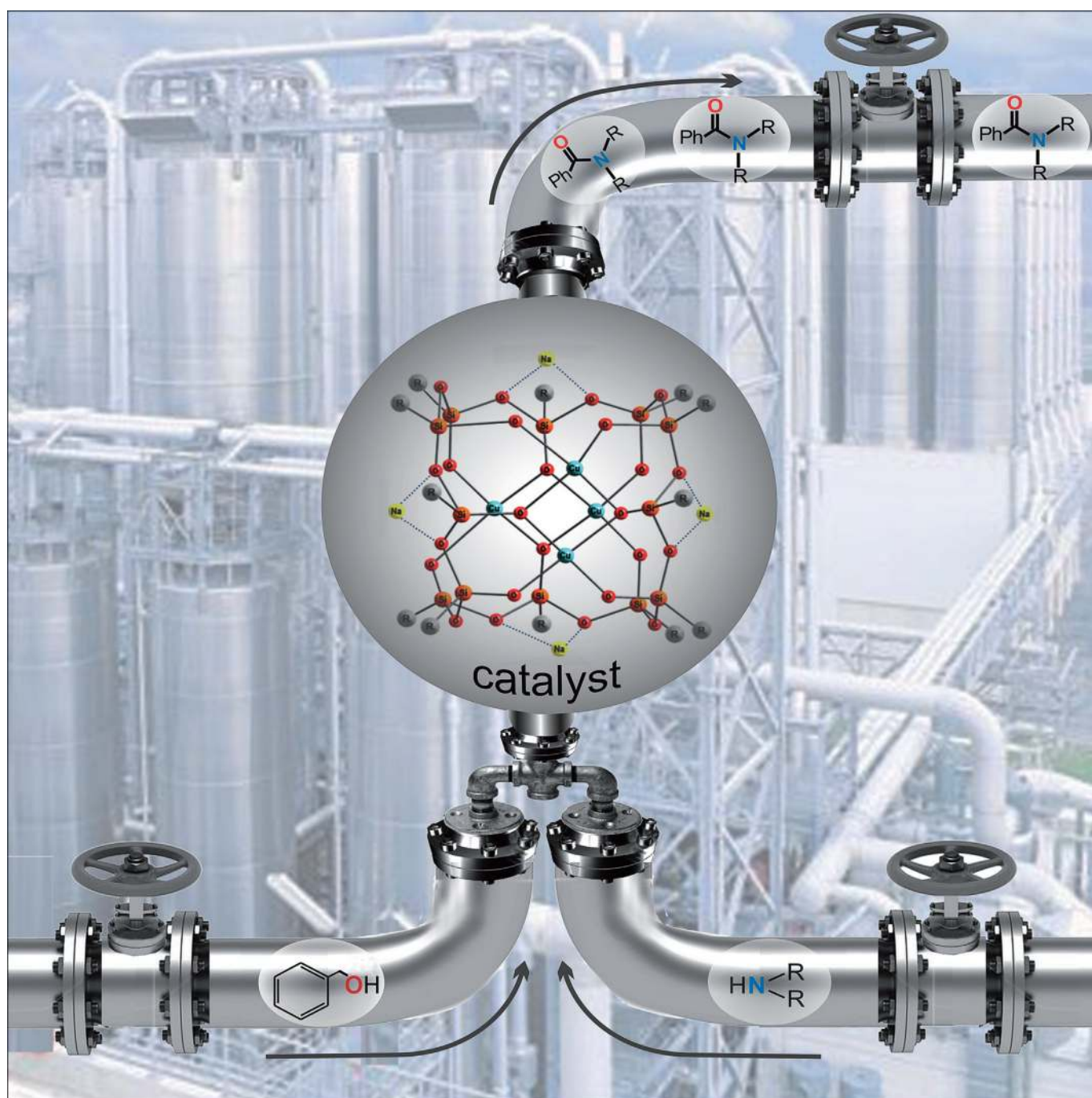
Abstract: The transmetalation of bimetallic copper–sodium silsesquioxane cages, namely, $[(PhSiO_{1.5})_{10}(CuO)_2(NaO_{0.5})_2]$ ("Cooling Tower"; **1**), $[(PhSiO_{1.5})_{12}(CuO)_4(NaO_{0.5})_4]$ ("Globule"; **2**), and $[(PhSiO_{1.5})_6(CuO)_4(NaO_{0.5})_4(PhSiO_{1.5})_6]$ ("Sandwich"; **3**), resulted in the generation of three types of hexanuclear cylinder-like copper silsesquioxanes, $[(PhSiO_{1.5})_{12}(CuO)_6(C_4H_9OH)_2(C_2H_5OH)_6]$ (**4**), $[(PhSiO_{1.5})_{12}(CuO)_6(C_4H_8O_2)_4(PhCN)_2(MeOH)_4]$ (**5**), and $[(PhSiO_{1.5})_{12}(CuO)_6(NaCl)(C_4H_8O_2)_{12}(H_2O)_2]$ (**6**). The products show a prominent "solvating system–structure" dependency, as determined by X-ray diffraction. Topological analysis of cages **1**–**6** was also performed. In addition, DFT theory was used to examine the structures of the Cooling Tower and Cylinder compounds, as well as the spin density distributions. Compounds **1**, **2**, and **5** were applied as catalysts for the direct oxidation of alcohols and amines into the corresponding amides. Compound **6** is an excellent catalyst in the oxidation reactions of benzene and alcohols.

Introduction

Cage-like metallasilsesquioxanes (CLMSs) represent an unusual class of compounds that simultaneously exhibit properties of both organosilicon derivatives and nanoscale metal clusters; thus attracting significant interest from scientific teams worldwide.[1] A unique feature of CLMSs is a combination of σ- and coordination-bonded compounds, which help to explain the huge variety of molecular architectures of CLMSs.[1a,f] The most abundant representatives of CLMSs are compounds based on the cubane-shaped silsesquioxane polyhedron, which have been discussed in detail in several reviews.[1b,c,e,g,h] The application of CLMSs, for example, as catalysts in different reactions, is therefore mostly limited to the use of cubane-like compounds,[1c,2] although the catalytic properties of CLMSs of non-cubane types have been described in a small number of publications.[3]

Recently, we presented a novel approach toward non-cubane CLMSs, containing copper and sodium ions, incorporated in silsesquioxane matrixes of dramatically varied shapes.[4]

[a] Dr. A. N. Bilyachenko, Dr. M. S. Dronova, A. I. Yalymov, L. S. Shul'pina, Prof. A. A. Korlyukov, D. E. Arkhipov, Dr. M. M. Levitsky, Prof. E. S. Shubina
Nesmeyanov Institute of Organoelement Compounds
Russian Academy of Sciences, Vavilov str., 28
Moscow 119991 (Russia)
E-mail: bilyachenko@ineos.ac.ru
    alex@xrlab.ineos.ac.ru
    levitsk@ineos.ac.ru

[b] Dr. F. Lamaty, Dr. X. Bantreil, Prof. J. Martinez, C. Bizet
Institut des Biomolécules Max Mousseron (IBMM)
UMR 5247 CNRS–Université Montpellier-ENSCM
Bâtiment Chimie (17), Faculté des Sciences Place
Eugène Bataillon 34095 Montpellier cedex 5 (France)
E-mail: frederic.lamaty@univ-montp2.fr

[c] Prof. A. A. Korlyukov
Pirogov Russian National Research Medical University
Ostrovitianov str., 1, Moscow 117997 (Russia)

[d] Dr. A. M. Kirillov
Centro de Química Estrutural, Complexo I
Instituto Superior Técnico, Universidade de Lisboa
Av. Rovisco Pais, 1049-001 Lisbon (Portugal)

[e] Prof. G. B. Shul'pin
Semenov Institute of Chemical Physics, Russian Academy of Science
ul. Kosygina, dom 4, Moscow 119991 (Russia)
E-mail: shulpin@chph.ras.ru

These compounds were revealed to be capable of effectively catalyzing the oxygenation of hydrocarbons and alcohols.[4]

The oxidation of hydrocarbons, alcohols, and other C—H compounds with peroxides in the presence of metal complexes represents an important field of contemporary metal-complex catalysis.[5] In particular, given the presence of copper ions in the active sites of various oxidizing enzymes,[6] a high diversity of biomimetic or bioinspired copper-based catalytic systems have been developed for the oxidation of C—H bonds by peroxides.[7] Different copper derivatives also catalyze the oxidation reactions of alcohols[8] and aromatic compounds.[9] Bearing this in mind, we were interested in studying these new types of copper-containing cage silsesquioxanes as catalysts in oxidation reactions. Because our prior studies were devoted to the investigation of bi- and tetranuclear copper cage silsesquioxane compounds,[4] it seemed particularly interesting to evaluate the activity of bigger clusters and to discuss the possible influence of nuclearity on catalytic activity.

Also, ruthenium-[10] and rhodium-catalyzed[11] direct oxidation of alcohols and amines into the corresponding amides has attracted much attention, and some methodologies involving cheap transition metals (Mn, Zn, Cu, and Fe) and *tert*-butyl-hydroperoxide as a terminal oxidant have recently been developed.[12] However, CLMSs containing such cheap transition-metal ions have never been evaluated as catalysts in these amidation reactions.

This paper is devoted to a comprehensive study of several types of cage-like copper silsesquioxanes, including their synthesis, structural and topological analysis, and quantum chemical studies. Some of these compounds were also evaluated as catalysts for amide production, as well as in oxidation reactions of benzene and alcohols with peroxides.

Results and Discussion

Synthesis

Synthetic approaches to CLMSs include several examples of transmetalation of different cages,[13] but none of them describe transformations of structurally distinct cages under conditions of total replacement of alkaline-metal ions by polyvalent ones.

Recently, we reported the synthesis and structural analysis of three types of cage-like Cu,Na-phenylsilsesquioxanes ("Cooling

Tower" (**1**), "Globule" (**2**), and "Sandwich" (**3**)),[4a,b] which show significant differences in molecular architecture and composition. A common feature of all of these compounds is the presence of silanolate (RSi−O−Na) fragments, which seem to be suitable sites for transmetalation reactions due to their high reactivity. To probe the possibility of such a procedure, we attempted to replace sodium ions in the "initial" cages **1**–**3** with copper ones. The treatment of copper–sodium silsesquioxanes **1**–**3** with copper chloride led to a new family of hexanuclear products **4**–**6** with cylinder-like structures (Figure 1). Complexes **4**–**6** (Figures 2–4) contain three six-membered cycles: two siloxanolate cycles and one metal oxide ring lying between them. The cylinder-like form of the products is different from the shape of the initial cages, which is especially clear in cases of the transformation of the decasilsesquioxane skeleton of compound **1**[4a] and dodecasilsesquioxane skeleton of compound **2**[4b] into two six-membered silsesquioxane units of products **4**–**6**. Deep structural reorganization, which accompanies transmetalation, could not be denied, even in the case of reactions involving **3**. Formally, organosilicon components of this compound (two six-membered siloxanolate cycles) are the same as those observed in cylinder-like products **4**–**6**. However, the copper-containing core of compound **3** (two metal oxide Cu_2O_2 cycles in an eclipsed conformation with respect to each other[4b]) is different from the almost planar configuration of metal oxide Cu_6O_6 cycles in **4**–**6**. In summary, it might be said that all transmetalation reactions reflect the phenomenon of significant rearrangement of cages. Nevertheless, all products of transmetalation are characterized by a common set of
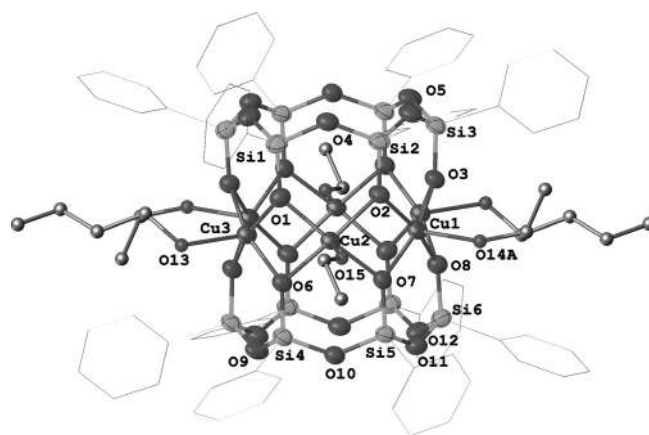
Figure 2. Copper silsesquioxane structure **4**. Atoms are drawn by ADP ellipsoids at 50% probability. Phenyl groups and the carbon atoms of EtOH and *n*BuOH are schematically shown by wireframe and stick representations. For a representation in color see the Supporting Information.

important parameters: compounds **4**–**6** are hexanuclear, whereas the atomic ratio of silicon/copper is equal to 2/1 (this ratio is equal to 5/1 and 3/1 for compounds **1** and **2**–**3**, respectively). The type of product nuclearity was independent not only of structural variety of the initial compounds, but also of the solvent system of the reaction (see the Experimental Section).

It seems that the observed formation of hexanuclear cylinder-like products is not exclusive. One of us reported the first
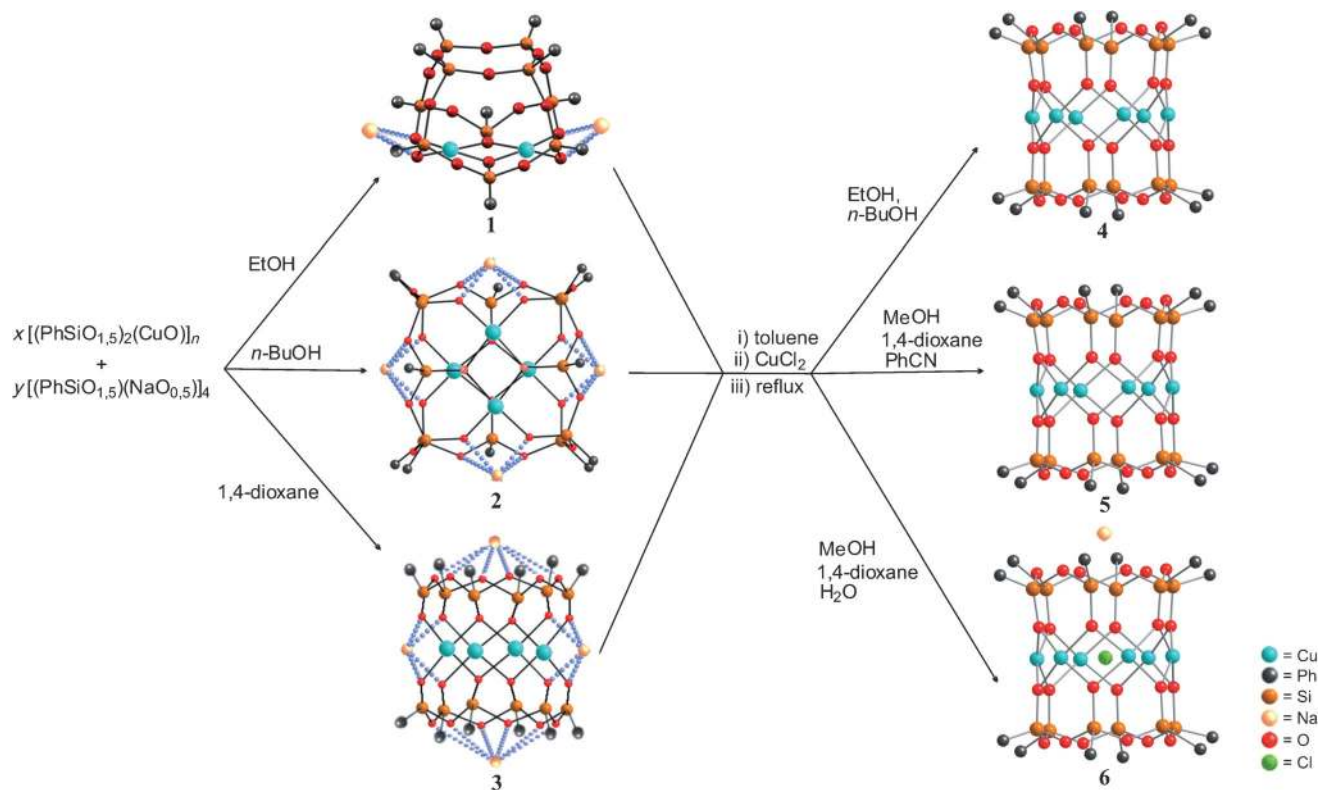
Figure 1. General scheme for the synthesis of the initial (**1**–**3**) and resulting (**4**–**6**) copper phenylsilsesquioxanes.
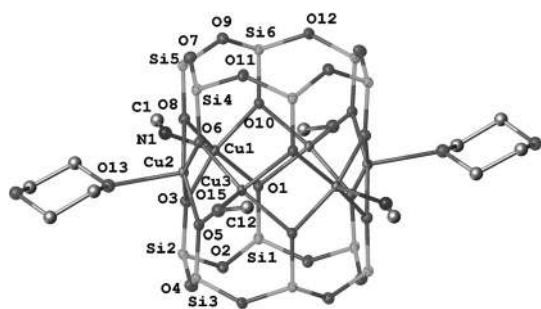
Figure 3. Copper silsesquioxane structure **5**. Atoms of copper silsesquioxane are drawn by atomic displacement parameter (ADP) ellipsoids at 50% probability. Phenyl groups and 1,4-dioxane moieties are schematically shown by a wireframe representation. For a representation in color see the Supporting Information.
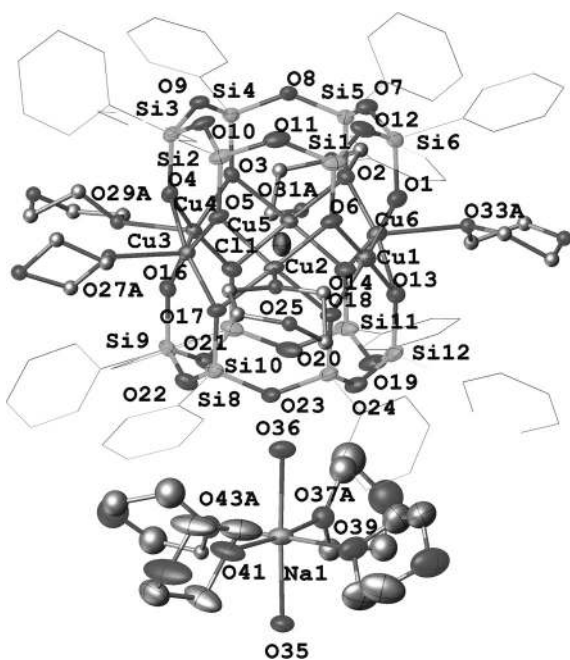

Figure 4. Copper silsesquioxane structure **5**. Atoms of copper silsesquioxane are drawn by ADP ellipsoids at 50% probability. Phenyl groups and 1,4-dioxane moieties are schematically shown by a wireframe representation. For a representation in color see the Supporting Information.

instance of the formation of similar hexanuclear compounds (containing Cu^{II}, Mn^{II}, and Co^{II} ions).[14] This report described an alternative synthetic approach and, what now seems to us to be very important, described the use of other solvent systems than those reported herein. It might be concluded that the formation of hexanuclear products is characteristic of synthetic conditions under which sodium ions of the silanolate fragments are completely replaced by copper(II) ions, even if such replacement is accompanied by the deep rearrangement of the silsesquioxane skeletons.

It is important to note that the use of a small amount of water during the synthesis of **6** (see the Experimental Section) allowed us to obtain an unusual, cage-like, copper-containing compound that encapsulated a chloride anion. Clearly, the presence of extra water in the reaction medium prevented the

complete removal of side product (NaCl) and led to the first instance of anion encapsulation in copper silsesquioxane cage compounds. This provoked significant contraction of the skeleton of cage **6** through the additional coordination of copper ions with the μ_6-Cl$^-$ ligand. A more detailed discussion of this fact (as well as the early unknown phenomenon of the structural sensitivity of hexacopper dodecasilsesquioxane cages toward the solvating ligand system as the whole) is provided below.

Structural considerations

The structures of **4–6** were determined by single-crystal XRD (Table 1). The most interesting feature of these compounds is significant structural susceptibility of the cylindrical shape of

Table 1. Average values of selected structural parameters of **4–6** (numbering is shown in Figure 5).

Structural parameter	4	5	6
Cu—O$_1$	2.005	2.006	1.990
Si—O$_1$	1.608	1.613	1.613
Si—O$_2$	1.622	1.629	1.631
$d_{1\cdots2}$	2.822	2.858	2.756
$d_{1\cdots4}$	5.696	5.714	5.557
Cu-O-Cu	88.1	86.7	88.3

the copper silsesquioxane cage, as governed by the solvates, surrounding the metallasilsesquioxane skeleton of the complex. The influence of coordinated solvent molecules can be studied by considering the distances between opposite copper atoms (distances $d_{1\cdots4}$, see Figure 5 for details). In the case of structure **4**, these distances are equal to 5.760, 5.573, and 5.755 Å, which correspond to almost an undistorted cylindrical shape of the hexacopper dodecaphenylsilsesquioxane moiety (Figure 2).[15]
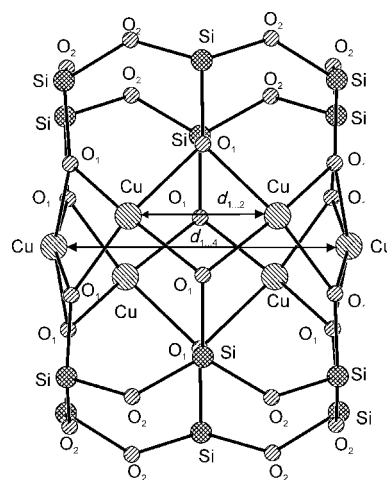
Figure 5. Schematic representation of a cylinder-like hexacopper dodecaphenylsilsesquioxane.

Distortion of the cage moiety becomes prominent in the case of complex **5** (Figure 3), in which $d_{1...4}$ are equal to 5.915, 5.547, and 5.679 Å. The reason for such a pronounced distortion of the cylindrical shape is probably related to the replacement of solvent molecules (from those almost equal in their donor ability, *n*BuOH and EtOH in **4**, to PhCN, MeOH, and 1,4-dioxane in **5**). It should be emphasized that compound **5** is the first example of the successful use of a benzonitrile ligand for the stabilization of a metallasilsesquioxane cage. Nevertheless, the structure of **6** (Figure 4) is even more remarkable because it allows us to discuss the influence of anion (Cl⁻) encapsulation in copper silsesquioxane cage compounds. First, the presence of Cl⁻ in **6** leads to a noticeable contraction of the inner void of the cage ($d_{1...4}$ distances are equal to 5.582, 5.458, and 5.631 Å). Interestingly, the position of the chloride anion is not exactly at the inversion center of the cage structure. The chloride anion is shifted toward the Cu1 atom (the Cu1···Cl1 distance is 2.669 Å). Hence, there is a pronounced alteration of distances between vicinal copper atoms ($d_{1...2}$). The shortest $d_{1...2}$ is Cu1···Cu6 (2.714 Å), whereas the longest one is Cu3···Cu4 (2.809 Å). Charge neutrality of the entirety of compound **6** is maintained by an external sodium cation, which is coordinated by the siloxanolate cycle.

Topological analysis

To gain a further insight into the structural features of copper silsesquioxane derivatives **1**–**6** with various cluster motifs, we performed a topological classification. It should be mentioned that the topological classification of silsesquioxane cage-like compounds has not been reported previously. Compounds **1**, **2**, and **3** reveal 2C1, (1,2M4-1)$_2$, and 2M6-1 topology, respectively (for details, see the Supporting Information), and the analysis of new derivatives **4**–**6** is described below.

For the sake of topological classification of the discrete 0D Cu$_6$ clusters in **4** and **5**, we have applied a method developed for the topological analysis of high nuclearity coordination clusters.[16] As a representative example, the analysis of **5** is described in detail. Thus, its simplified structure (Figure 6a) was generated by removing all non-metal atoms, except for the oxygen bridges between the copper centers. Then, a graph representation of the Cu$_6$ skeleton (Figure 6b) was obtained after transforming all of the μ$_2$-O atoms (Cu-O-Cu) into Cu–Cu edges. Topological analysis of the resulting 2-connected 0D net reveals the 2M6-1 topology.[16a] This topology is described by the *NDk-m* classification, wherein *N* is a set of coordination numbers of the topologically nonequivalent nodes (*N* = 2 for 2-connected nodes), D is dimensionality (D = M for discrete 0D molecular clusters), *k* is the number of metal atoms in the cluster (*k* = 6), and *m* is a classification number to distinguish topologically distinct clusters with equal *NDk* parameters.[16b, 17] Compound **4** possesses the same 2M6-1 topology and thus is not discussed further.

An interesting feature of **5** consists of the extension of discrete 0D Cu$_6$ units into a 2D hydrogen-bonded network through intermolecular O15—H15···O16 and O16—H16···O2 hydrogen bonds between the MeOH ligand (O15) and solvent
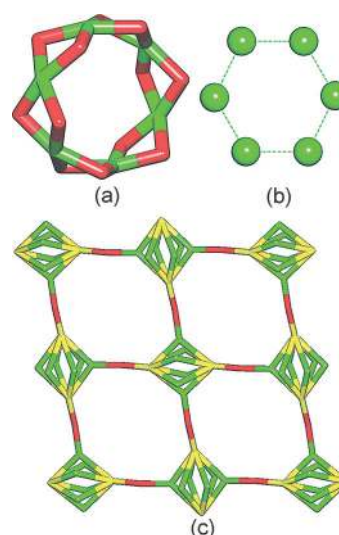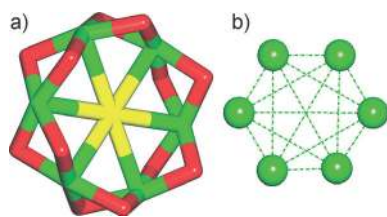

Figure 6. Topological fragments of **5**: a) a discrete Cu$_6$ coordination cluster and b) its simplified graphical representation, showing a uninodal 2-connected motif with the 2M6-1 topology; c) an underlying binodal 3,4-connected 2D hydrogen-bonded net with the 3,4L27 topology and point symbol of $(3.8^2)(3^2.4.8^2.9)$. Color codes: a) Cu centers (green), μ$_2$-O atoms (red); b) 2-connected Cu nodes (green); c) 2-connected Cu1/Cu2 linkers and 3-connected Cu3 nodes (green), centroids of 4-connected silsesquioxane nodes (yellow), and centroids of 2-connected (MeOH)$_2$ linkers (red).

(O16) molecules (forming a dimeric MeOH cluster) and the O2 atom of the silsesquioxane moiety. To better understand the structure of the resulting 2D hydrogen-bonded layer, we carried out its topological analysis[16a] by following the concept of the simplified underlying net.[17, 18]

A different structure simplification strategy was applied.[16a, 18b,c] The terminal cyanobenzene ligands were eliminated and the bridging silsesquioxane and (MeOH)$_2$ moieties were contracted to their centroids; thus giving an underlying network (Figure 6c) composed of the 3-connected Cu3 and 4-connected silsesquioxane nodes, as well as 2-connected Cu1, Cu2, and (MeOH)$_2$ linkers. Its topological analysis discloses a binodal 3,4-connected net with the 3,4L27 topology and the point symbol of $(3.8^2)(3^2.4.8^2.9)$, wherein the (3.8^2) and $(3^2.4.8^2.9)$ notations are those of the Cu3 and silsesquioxane nodes, respectively. A number of 3,4L27 topological networks driven by copper nodes have been reported.[19] It is noteworthy to mention that the present net can be simplified further by treating the Cu$_6$(silsesquioxane)$_2$ blocks as 4-connected cluster nodes, which, along with the (MeOH)$_2$ linkers, give rise to a uninodal 4-connected network with the **skl** (Shubnikov tetragonal plane net) topology described by the point symbol of $(4^4.6^2)$.

In contrast to **4** and **5**, the structural core of 0D Cu$_6$ coordination cluster **6** is more complex due to the presence of the "central" μ$_6$-Cl moiety (Figure 7a). Following the above-mentioned procedure,[16a,b] we also obtained a graph representation of the Cu$_6$ skeleton (Figure 7b), namely, by transforming the μ$_2$-O atoms (Cu-O-Cu) into Cu–Cu edges and contracting the μ$_6$-Cl atom into Cu nodes to retain the cluster connectivity.[16a,b] The resulting skeleton has been topologically classified as a

Figure 7. Topological fragments of **6**: a) a discrete Cu₆ coordination cluster and b) its simplified graph representation showing a uninodal 5-connected motif with the 5M6-1 topology. Color codes: a) Cu centers (green), μ_2-O atoms (red), μ_6-Cl atom (yellow); b) 5-connected Cu nodes (green).

uninodal 5-connected net with the 5M6-1 topology (*NDk-m* classification). No topologically relevant hydrogen-bonding interactions were observed in **6**.

In summary, the performed analysis resulted in the topological classification of copper-containing silsesquioxane cages and their extended networks in compounds **1**–**6**, which allowed the identification of diverse topological motifs. We believe that these results can contribute to the prediction of novel metal silsesquioxane cages and facilitate their design and synthesis.[16b,c,17,18]

Quantum chemical calculations

To the best of our knowledge, quantum chemical calculation on CLMSs is the rarest type of such modeling.[20] Possibly, the realization of such calculations was constrained by the huge size of such clusters. In turn, quantum chemical calculations may be useful to reveal the electronic structure of these compounds. Unfortunately, a direct comparison for cage compounds, as discussed herein, is possible only for binuclear silsesquioxane **1**, in which the spin-coupling constant can be calculated by the broken symmetry approach as the difference between triplet and singlet states.

To study the features of the electron structure of **1** (Figure 8) and the cylinder compound (Figure 5), quantum chemical calculations in the framework of DFT theory were carried out. The optimization of **1** started from experimental coordinates.[4a] Initial coordinates for the optimization of different forms of the cylinder (with or without an encapsulated chloride anion) were taken from the results of X-ray structure determinations of compounds **6** and **5**, respectively. The main structural para-
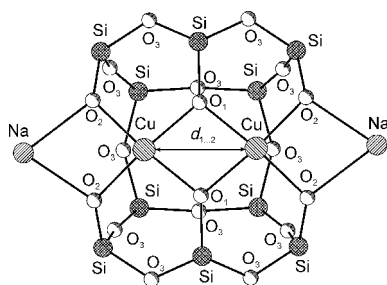
Figure 8. Schematic representation of the structure of **1**.

Table 2. Mean values of bond lengths [Å] and angles [°] for the calculated structure of binuclear silsesquioxane **1**. The experimental values from the literature[4a] are also given. The numbering of atoms is shown in Figure 8.

	Experimental values	Singlet	Triplet
Cu–O1	1.954	1.996	1.989
Cu–O2	1.910	1.960	1.941
Si–O1	1.626	1.656	1.662
Si–O2	1.606	1.630	1.632
Si–O3	1.620	1.667	1.669
$d_{1\cdots2}$	2.997	2.819	3.014
Cu-O-Cu	100.2	89.9	98.5

Table 3. Selected parameters for the calculated structure of the cylindrical compound (the numbering of atoms is shown in Figure 5).

	Singlet	Triplet	Quartet	Quintet
bond length and angles [Å]				
Cu–O1	1.962	1.967	1.961	1.961
Si–O1	1.679	1.668	1.673	1.672
Si–O2	1.662	1.657	1.662	1.661
$d_{1\cdots2}$	2.706/2.949	2.774	2.764	2.748
$d_{1\cdots4}$	5.654	5.549	5.518	5.497
Cu-O-Cu	87.3/97.4	89.7	89.4	89.0
spin population [e]				
Cu		0.60	0.61	0.61
O1		0.15	0.15	0.15
atomic charges [e]				
Cu	0.24	0.26	0.26	0.26
O1	−0.23	−0.24	−0.24	−0.24
O2	−0.25	−0.25	−0.25	−0.25

Table 4. Selected parameters for the calculated structure of the cylinder compound with an encapsulated chloride anion (numbering of atoms is shown in Figure 5).

	Singlet	Triplet	Quartet	Quintet
bond length and angles [Å]				
Cu–O1	1.987	1.990	1.990	1.991
Si–O1	1.668	1.664	1.664	1.663
Si–O2	1.664	1.661	1.661	1.661
Cu···Cl	2.824	2.754	2.752	2.748
$d_{1\cdots2}$	2.822	2.756	2.752	2.748
$d_{1\cdots4}$	5.652	5.508	5.503	5.495
Cu-O-Cu	90.5	87.6	87.5	87.3
spin population [e]				
Cu		0.61	0.63	
O1		0.15	0.15	
Cl		0.005	0.011	0.016
atomic charges [e]				
Cu	0.21	0.23	0.23	0.23
O1	−0.23	−0.24	−0.24	−0.25
O2	−0.25	−0.25	−0.25	−0.25
Cl	−0.18	−0.14	−0.14	−0.14

meters, spin populations, and charges of atoms are presented in Tables 2–4.

The optimization of atomic positions of **1** was carried out for singlet and triplet states. Analogously, the cylinder-like

compound was optimized in the singlet ($S=0$), triplet ($S=1$), quartet ($S=2$), and quintet states ($S=3$).

The structural parameters of **1** in the singlet state are different from those of the triplet state. Remarkably, the value of $d_{1\cdots2}$ in the triplet state is 0.2 Å larger than that in the singlet state. The Cu-O-Cu angles in the triplet and singlet states are 89.9 and 98.6 ° on average. At the same time, the lengths of the Cu—O bonds in the singlet and triplet states differ by less than 0.02 Å. Thus, the optimized structure of **1** in the triplet state is closer to the experimental one than the structure of the singlet state. To analyze the spin population of atoms, we used the method based on Hirschfield partitioning of electron density. The spin populations of copper atoms are 0.62 e, whereas their atomic charges are equal to 0.24 e. The rest of the spin density is distributed over bridge oxygen atoms O_1 and terminal oxygen atoms O_2 (the values of the spin population are 0.15 and 0.09 e).

The structural parameters of various spin states of the cylinder compound are also noticeably different. The most prominent feature of the structure of the singlet state is the alteration of the $d_{1\cdots2}$ distances. The short $d_{1\cdots2}$ contacts alternate to long $d_{1\cdots2}$ ones (2.70 and 2.95 Å, on average). In the structure of the triplet state there is no visible change to the above distances; however, the $d_{1\cdots2}$ contacts varied over a rather wide range (2.741–2.795 Å). The states with higher multiplicity ($S=2$ and 3) are characterized by the absence of alteration of the $d_{1\cdots2}$ distances (the variations do not exceed 0.02 Å). Thus, the geometry of the quartet and quintet states is in better agreement with that determined experimentally than states with low spin ($S=0$ and 1). Regardless of the spin state, the atomic spin population of the copper atom is about 0.6 e, whereas the spin population of bridge oxygen atom O1 is 0.15 e. The spin populations of the rest of atoms are negligible.

The inclusion of a chloride anion into the inner cavity of the cylinder compound (in the case of product **6**) leads to the absence of changes to the $d_{1\cdots2}$ distances in the singlet state observed in the case of the chloride-less analogue. Indeed, the chloride anion in the optimized geometry is located at the center of inversion, regardless of the spin state, so all Cu···Cl distances are equal. The increase in the total multiplicity of the chloride-containing form of the cylinder lead to a decrease in the value of $d_{1\cdots2}$, so the value for the quintet state differs from that of the singlet state by 0.06 Å. Additionally, quantum chemical calculations reproduced the contraction of the inner cavity upon inclusion of the chloride anion. The values of the $d_{1\cdots4}$ distances in the calculated structures of the quartet states are very close to those obtained experimentally. Analysis of the spin density distribution showed that the population at the Cl atom was very small (0.02 e), whereas the values for copper and bridge oxygen atoms are the same (0.63 and 0.15 e, respectively) as those in the cylinder compounds without inclusion of a chloride anion.

Catalytic oxidation of benzylic alcohols into amides

Some of us recently reported copper-catalyzed benzamide formation directly from alcohols and amine hydrochlorides.[12e]

Herein, we present the first example of the evaluation of CLMSs under these amidation conditions. Such a reaction was originally performed with 2 mol% of CuO in the presence of *tert*-butylhydroperoxide (TBHP) in acetonitrile at reflux. To take advantage of the good solubility of cage coppersilsesquioxanes in organic solvents, stock solutions of the catalysts were prepared in acetonitrile, which allowed us to work with a very low catalyst loading. It is important to note that CLMSs act as the precatalyst and that the structure might be partly changed under the reaction conditions. Optimization of the reaction conditions was performed with compound **1**. When the reaction was carried out under the reported conditions starting from benzyl alcohol (**7a**) and (α)-methyl benzylamine hydrochloride (**8a**),[12e] but with only 100 ppm of copper in acetonitrile at reflux for 24 h, product **9aa** was isolated in 99% yield (Table 5, entry 1). Because a very low catalyst loading in copper

Table 5. Optimization of the reaction conditions.[a]

Entry	Catalyst	Cu [mol%]	Base	Yield [%]	TOF [h^{-1}][b]
1	**1**	0.01	CaCO$_3$[c]	99	413
2	**1**	0.01	CaCO$_3$	72	300
3	**1**	0.01	–	35	146
4	–	–	CaCO$_3$	24	–[d]
5	**1**	0.005	CaCO$_3$	58	483
6	**1**	0.01	CaCO$_3$	83[e]	346
7	**1**	1	CaCO$_3$	84[e]	21
8[f]	CuO	2	CaCO$_3$[c]	87	11

[a] Reaction conditions: **8a** (0.5 mmol), **7a** (0.75 mmol), CaCO$_3$ (99.995% pure; 0.5 mmol), TBHP (5.5 M in nonane, 5 equiv, 2.5 mmol), CH$_3$CN (1 mL), 80 °C, 24 h. [b] Turnover frequency (TOF) = (mmol of product)/[(mmol of Cu)(reaction time)]. [c] CaCO$_3$ 99% pure was used. [d] Not relevant. [e] Two equivalents of **7a** were used. [f] Result taken from the literature.[12e]

was used, metallic impurities contained in the inorganic base would be able to perform and enhance the amidation reaction. Indeed, in the presence of CaCO$_3$ (99.995% pure), amide **9aa** was isolated in 72% yield, which proved that traces of metal were present in the first batch of base used (Table 5, entry 2). In view of these latest results, 99.995% pure CaCO$_3$ was used in the rest of the study. Control experiments showed that base and copper were indispensable for this reaction (Table 5, entries 3 and 4). Diminishing the catalyst loading to 50 ppm of copper gave 58% yield, which indicated that 100 ppm might be the bottom limit for this reaction (Table 5, entry 5). To obtain an even higher yield of **9aa** with only 100 ppm of copper as the catalyst, the stoichiometry of **7a** was increased to 2 equivalents. Gratifyingly, amide **9aa** was isolated in 83% yield (Table 5, entry 6). A remarkable point was that amide **9aa** could be obtained in similar yield whether 1 mol% or 100 ppm of copper was used (Table 5, entry 7); thus proving that using

such a low catalyst loading did not influence the outcome of the reaction. In addition, compared with the original report with CuO (Table 5, entry 8), our new set of conditions was superior in terms of turnover number (TON; 8300 vs. 44) and TOF (346 vs. 11 h^{-1}).

To ensure that such a low catalyst loading would be generally efficient and to compare the various CLMSs, as a first approach, we chose three of the six catalysts containing two, four, and six copper centers, namely, compounds **1**, **2**, **5**, and performed tests by varying the amine. Primary amines, with varying steric hindrance, and secondary amines were tested (Table 6). Compared with the original report involving CuO (2 mol%), amides **9aa**–**9af** were isolated in at least similar yields when only 100 ppm of Cu was used. Benzamides **9aa**, **9ab**, and **9ac**, featuring primary (α)-methylbenzylamine, cyclohexylamine, and n-butylamine, respectively, were isolated in yields of up to 94% (Table 6, entries 1–12). Dibenzylamine, piperidine, and morpholine were efficiently converted into the corresponding amides **9ad**, **9ae**, and **9af**, with yields from 64 to 93% (Table 6, entries 13–24). According to these results, it is apparent that working with CLMSs at very low catalyst loading gives outstanding results. Nevertheless, if CLMSs **1**, **2**, and **5** were efficient in the amidation reaction, catalyst **2**, which

featured four copper centers, was slightly superior to its congeners (Table 6, entries 2, 14, 18, and 22). These good results, combined with a very low catalyst loading, translated directly into the TON and TOF values obtained. Indeed, excellent TON and TOF values, reaching 9400 and 392 h^{-1}, respectively, were calculated for this amidation reaction.

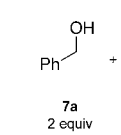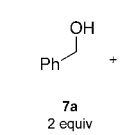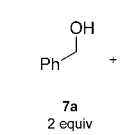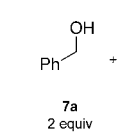## Catalytic oxidations of benzene and alcohols
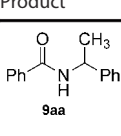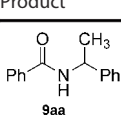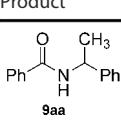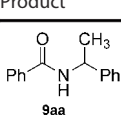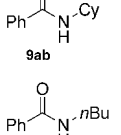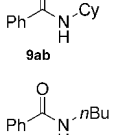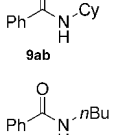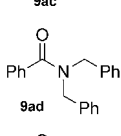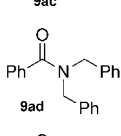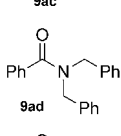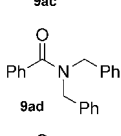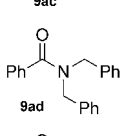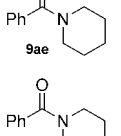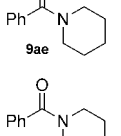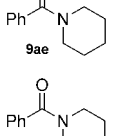
We tested compounds **5** and **6** as catalysts in the oxidation of benzene, hydroquinone, and 1-phenylethanol with aqueous hydrogen peroxide. Herein, we report the first results of this study.

Benzene was oxidized to produce phenol, which at high concentrations of the catalysts is further nonselectively transformed into overoxidation products, including p-quinone (Figure 9). The reaction required the presence of a small amount of an acid promoter (Figure 9a, curve 1, and Figure 9b, curve 1). Thus, nitric acid added to the reaction solution substantially improved the reaction catalyzed by **6** (Figure 9b). However, the use of nitric acid resulted in the degradation of catalyst **5**, which slowly precipitated as a pale-blue solid during the course of the reaction. Fortunately, this was not the case with TFA and the reaction afforded 0.05 M of phenol after 2.5 h (Figure 9a). Nevertheless, compound **6** (in the presence of nitric acid) catalyzed the oxidation noticeably more efficiently to give phenol in a concentration of 0.08 M after 1 h (yield of 18% based on starting benzene; TOF = 160 h^{-1}; Figure 9b, curve 5). It is interesting to note that the initial oxidation rate, W_0, linearly depends on the concentration of **6** in the interval of its concentrations $(0–3)\times10^{-4}$ M (Figure 9c). In the absence of TFA or HNO$_3$, oxidation is not efficient (Figure 9a, curve 1, and Figure 9b, curve 1).

Several experiments with varying initial concentrations of benzene, hydrogen peroxide, and nitric acid were carried out. A linear dependence of the initial reaction rate, W_0, on the initial concentration of benzene has been found for benzene concentrations in the interval [benzene]$_0$ = 0–0.3 M (Figure S1, curve 1, in the Supporting Information). At higher benzene concentrations the curve approaches a plateau. Additionally, the dependence of W_0 on the initial concentration of hydrogen peroxide (containing 65% of water) has 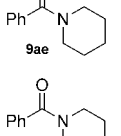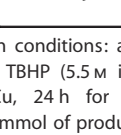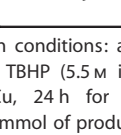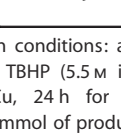the shape of a parabola (Figure S1, curve 2, in the Supporting Information). The initial reaction rate at [HNO$_3$] > 0.03 M was independent of the concentration of added nitric acid (Figure S2, curve 1, in the Supporting Information). Finally, the addition of water slightly decreases the initial oxidation rate (Figure S2, curve 2, in the Supporting Information).

All of these observations showed that the kinetic behavior of the copper-based systems described above resembled the features of benzene oxidation with the vanadate anion/pyrazine-2-carboxylic acid

Table 6. Variation of the amine at low catalyst loading.[a]

Entry	Product	Catalyst	Cu [mol%]	Yield [%]	TON/TOF[b,c]
1	9aa	1	0.01	83	8300/346
2		2	0.01	94	9400/392
3		5	0.01	71	7100/296
4		CuO[d]	2	87	44/11
5	9ab	1	0.01	83	8300/346
6		2	0.01	83	8300/346
7		5	0.01	87	8700/363
8		CuO[d]	2	80	40/10
9	9ac	1	0.01	73	7300/304
10		2	0.01	74	7400/308
11		5	0.01	79	7900/329
12		CuO[d]	2	66	33/8
13	9ad	1	0.01	75	7500/313
14		2	0.01	93	9300/388
15		5	0.01	85	8500/354
16		CuO[d]	2	87	44/11
17	9ae	1	0.01	67	6700/279
18		2	0.01	71	7100/296
19		5	0.01	64	6400/267
20		CuO[d]	2	70	35/9
21	9af	1	0.01	71	7100/296
22		2	0.01	76	7600/317
23		5	0.01	66	6600/275
24		CuO[d]	2	62	31/8

[a] Reaction conditions: amine·HCl (0.5 mmol), **7a** (1.0 mmol), CaCO$_3$ (99.995% pure; 0.5 mmol), TBHP (5.5 M in nonane, 5 equiv, 2.5 mmol), CH$_3$CN (1 mL), 80°C, 4 h for 1 mol% Cu, 24 h for 0.01 mol% Cu. Yields of products isolated are given. [b] TON = (mmol of product)/(mmol of Cu). [c] TOF = TON/(reaction time); given in h^{-1}. [d] Calculated from data in the literature.[12e]
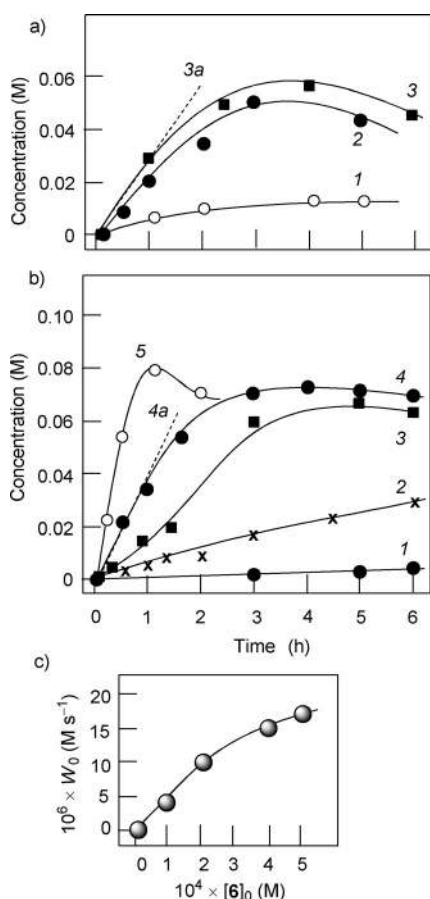
Figure 9. Oxidation of benzene to form phenol, as catalyzed by compounds **5** and **6** in acetonitrile at 50 °C. a) Kinetic curves of phenol accumulation in the oxidation of benzene (0.45 M) with H_2O_2 (2.6 M; 35% aqueous) catalyzed by **5** at 2×10^{-4} (curves *1* and *3*) and 1×10^{-4} M (curve *2*). b) Kinetic curves of phenol accumulation in the oxidation of benzene (0.45 M) with H_2O_2 (2.6 M; 35% aqueous) in the presence of HNO_3 (0.04 M, 65%) catalyzed by **6** at 0.5×10^{-4} (curve *2*), 1×10^{-4} (curve *3*), 2×10^{-4} (curve *4*; the analogous reaction in the absence of HNO_3 is shown by curve *1*), and 5×10^{-4} M (curve *5*). At $[\mathbf{6}]_0 = 0.5 \times 10^{-4}$ M (curve *2*) after 13 h, TON was 1510, TOF = 116 h^{-1}. The initial rates, W_0, were determined from the slope of the tangent (in certain examples shown as dotted straight lines *3a* and *4a*) to the kinetic curve of oxygenate accumulation. c) Dependence of the initial reaction rate, W_0, on the initial concentration of **6** (for conditions of the experiments presented in b).

(PCA)/H_2O_2 reagent in acetonitrile.[21] Analogously, the following mechanism for benzene oxidation catalyzed by copper cages could be proposed. A copper(II) compound reacts first with a molecule of H_2O_2 to produce a copper(I) derivative ($Cu^{II} + H_2O_2 \rightarrow Cu^{I} + HOO^{\bullet} + H^{+}$), which generates hydroxyl radicals that interact with a second hydrogen peroxide molecule ($Cu^{I} + H_2O_2 \rightarrow Cu^{II} + HO^{\bullet} + HO^{-}$).[22] Phenol is further formed in this process through a sequence of stages that do not limit the oxidation rate:
$C_6H_6 + HO^{\bullet} \rightarrow C_6H_6(OH)^{\bullet}$, $C_6H_6(OH)^{\bullet} + O_2 \rightarrow C_6H_6(OH)(OO^{\bullet})$, and $C_6H_6(OH)(OO^{\bullet}) \rightarrow C_6H_5OH + HOO^{\bullet}$.
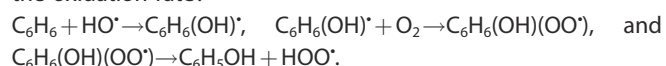
Compounds **5** and **6** were also tested as catalysts in the oxidation of hydroquinone at 20 °C. Compound **5** (Figure S3, curve 1, in the Supporting Information) oxidized hydroquinone to *p*-quinone less rapidly than compound **6** (Figure S3, curve 2,

in the Supporting Information), although the yield of quinone (56% after 4.5 h) in the case of **5** was higher. As observed above in the oxidation of benzene, neither reaction was efficient in the absence of TFA (Figure S3, curves 1a and 2a, in the Supporting Information). In the case of catalysts **5** or **6**, the formation of *p*-quinone was followed by its nonselective overoxidation to afford a complex mixture of unidentified compounds. As a result, the kinetic curves displayed maxima. Control experiments showed that hydroquinone could not be oxidized in the presence of only TFA in the absence of a copper catalyst (the concentration of quinone was 0.0013 M after 2 h) and especially in the absence of both TFA and a copper catalyst (in the presence of only hydrogen peroxide, the concentration of quinone was lower than 0.0001 M after 2 h).

Hydrogen peroxide turned out to be inefficient in the oxidation of 1-phenylethanol. In contrast, TBHP exhibited excellent activity. The reaction does not require the presence of any acid. Figure S4 in the Supporting Information demonstrates the accumulation of acetophenone over the course of the oxidation of 1-phenylethanol in the presence of TBHP catalyzed by **6** at 60 °C (95% yield after 5 h). It is interesting to note that, in contrast, compound **5** was unable to catalyze the oxidation of 1-phenylethanol with TBHP. Under the reaction conditions, compound **5** immediately precipitated as a pale-blue solid when TBHP was added.

Conclusion

Transmetalation of various copper–sodium phenylsilsesquioxanes (**1–3**) gave a family of three novel hexanuclear cage-like copper(II) silsesquioxanes (**4–6**), which exhibited noticeable structural flexibility as a consequence of different solvating systems used in the synthesis and crystallization. The most outstanding case among the hexanuclear products was compound **6**, which unusually trapped the chloride anion. The inclusion of Cl^- into the inner void of the copper silsesquioxane fragment led to a decrease of its volume owing to the presence of multiple Cu···Cl coordination bonds.

The current study also opens up the application of topological analysis methods for the classification of underlying networks in silsesquioxane derivatives. A topological analysis of the newly synthesized discrete Cu_6 coordination clusters revealed the uninodal 2- or 5-connected 0D skeletons with 2M6-1 (**4**, **5**) or 5M6-1 (**6**) topology, respectively. For comparison, compounds **1–3** were topologically classified. Thus, the same 2M6-1 topology was detected in complex **3** with the Cu_4Na_2 motif, whereas the compounds with the Cu_2Na_2 cores featured the 2C1 (**1**) and $(1,2M4-1)_2$ (**2**) topology. Furthermore, a noteworthy feature of **5** consists of the extension of its discrete units into the binodal 3,4-connected 2D hydrogen-bonded layer with 3,4L27 topology, which is similar to that identified in the metal–organic layer of **3**. The silsesquioxanes thus appear to be versatile building blocks for the construction of various multicopper(II) or copper–sodium cages. The structures of **1** and cylinder compounds were simulated by quantum chemical modeling; this is the first example of DFT calculations of

cage-like copper silsesquioxanes. According to results of the calculations, the experimental structure of **1** corresponded to the triplet state, so the spin density was distributed between copper atoms and bridged oxygen atoms. In turn, the geometry of the quartet and quintet states of the cylinder compound was in better agreement with the experimental one than states with low spin. Also, quantum modeling reproduced the contraction of the inner cavity of **6** upon inclusion of a chloride anion.

Compounds **1**, **2**, and **5** were evaluated in the direct oxidation of alcohols and amines into corresponding amides. All of these copper(II)-containing cages showed exceptional catalytic results, which allowed for an efficient reaction, even at copper loadings down to 100 ppm. Such behavior permitted TOF values to be obtained that ranged from 267 to 392 h^{-1}, which were much higher than the one reported so far in the literature for this type of reaction conditions (TOF < 34 h^{-1}).

Compound **6** turned out to be a very good catalyst for benzene oxidation with hydrogen peroxide in the presence of certain acids (nitric or trifluoroacetic). The oxidation of 1-phenylethanol with TBHP in the absence of acids was very effective to give an acetophenone yield close to 100%. Compound **5**, which does not contain any chloride anion connecting copper ions, is noticeably less stable and much less efficient as a catalyst. Further exploration of silsesquioxanes toward the design of copper–organic materials with intricate topologies and diverse functional properties is currently in progress.

Experimental Section

General procedures

All solvents were distilled prior to use according to standard procedures. Compounds **1**–**3** were obtained by following earlier published procedures.[4a,b] Elemental analyses were performed by the microanalytical service of the Nesmeyanov Institute of Organoelement Compounds RAS. IR studies on the dried solid samples were carried out as Nujol mulls on a Nicolet 6700 FTIR spectrometer in the 4000–600 cm^{-1} range. For initial and obtained copper(II)-containing silsesquioxanes, a usual set of signals (1120 (v^{Ph-Si}), 940–1100 (v_{as}^{Si-O}, $v_{as}^{Si-O-Si}$), 900 (v_{as}^{Si-O} in the Si-O-M fragment), 720–680 cm^{-1} (σ^{C-H} of monosubstituted phenyl group)) was observed.[4a,b]

Synthesis of 4

Compound 4a: Compound **1** (0.5 g, 0.33 mmol) was dissolved in toluene (25 mL). Then anhydrous CuCl₂ (0.044 g, 0.33 mmol) in a mixture of *n*-butanol (25 mL) and ethanol (15 mL) was added at once. The mixture was heated under reflux for 2.5 h, then cooled to room temperature, and filtered into an evaporation flask. The flask was equipped with a septum with needle to allow solvents to evaporate under a slow current of nitrogen. Immediately after blue-colored crystals began to form, the flask was transferred to the fridge and stored there until the crystal fraction growth (3–4 weeks) ceased, as visually determined. A few selected single crystals were used for the X-ray study (for details, see below). Yield: 0.16 g, 28%; elemental analysis calcd (%) for [(PhSiO₁.₅)₁₂(CuO)₆]: Cu 18.80, Si 16.62; found (in a vacuum-dried sample): Cu 18.59, Si 16.37.

Compound 4b: Compound **2** (0.5 g, 0.25 mmol) was dissolved in toluene (25 mL). Then anhydrous CuCl₂ (0.068 g, 0.5 mmol) in a mixture of *n*-butanol (25 mL) and ethanol (15 mL) was added at once. The mixture was heated under reflux for 2.5 h, then cooled to room temperature and filtered into an evaporation flask. The flask was equipped with a septum and needle to allow solvents to evaporate under a slow current of nitrogen. Immediately after blue-colored crystals began to form, the flask was transferred to the fridge and stored there until the crystal fraction growth (3–4 weeks) ceased, as visually determined. A few selected single crystals were used for the X-ray study (cell parameters equaled those of the product, as described for **4a**). Yield: 0.35 g, 69%; elemental analysis calcd (%) for [(PhSiO₁.₅)₁₂(CuO)₆]: Cu 18.80, Si 16.62; found (in a vacuum-dried sample): Cu 18.62, Si 16.34.

Compound 4c: The same procedure as that described for **4b** was used for the synthesis with compound **3** as an initial reagent. Yield: 0.37 g, 73%; elemental analysis calcd (%) for [(PhSiO₁.₅)₁₂(CuO)₆]: Cu 18.80, Si 16.62; found (in a vacuum-dried sample): Cu 18.54, Si 16.64.

Synthesis of 5

Compound 5a: Compound **1** (0.5 g, 0.33 mmol) was dissolved in a mixture of toluene (20 mL) and 1,4-dioxane (30 mL). The reaction mixture was brought to reflux and anhydrous CuCl₂ (0.044 g, 0.33 mmol) in methanol (20 mL) was added dropwise, along with simultaneous partial distillation of the solution. As 10 mL of solvents were distilled off, the rest of reaction mixture was down to room temperature and filtered into an evaporation flask containing benzonitrile (7 mL). The flask was equipped with a septum and needle to allow solvents to evaporate under a slow current of nitrogen. Immediately after blue-colored crystals began to form, the flask was transferred to the fridge and stored there until the crystal fraction growth (3–4 weeks) ceased, as visually determined. A few selected single crystals were used for the X-ray study (for details, see below). Yield: 0.14 g, 25%; elemental analysis calcd (%) for [(PhSiO₁.₅)₁₂(CuO)₆]: Cu 18.80, Si 16.62; found (in a vacuum-dried sample): Cu 18.59, Si 16.27.

Compound 5b: Compound **2** (0.5 g, 0.25 mmol) was dissolved in a mixture of toluene (20 mL) and 1,4-dioxane (30 mL). The reaction mixture was brought to reflux and anhydrous CuCl₂ (0.068 g, 0.5 mmol) in methanol (20 mL) was added dropwise, along with simultaneous partial distillation of the solution. As 10 mL of solvents were distilled off, the rest of reaction mixture was cooled to room temperature and filtered into an evaporation flask containing benzonitrile (7 mL). The flask was equipped with a septum and needle to allow solvents to evaporate under a slow current of nitrogen. Immediately after blue-colored crystals began to form, the flask was transferred to the fridge and stored there until the crystal fraction growth (3–4 weeks) ceased, as visually determined. A few selected single crystals were used for the X-ray study (cell parameters equaled those of the product, as described for **5a**). Yield: 0.37 g, 72%; elemental analysis calcd (%) for [(PhSiO₁.₅)₁₂(CuO)₆]: Cu 18.80, Si 16.62; found (in a vacuum-dried sample): Cu 18.69, Si 16.35.

Compound 5c: The same procedure as that described in **5b** was used for the synthesis with compound **3** was an initial reagent. Yield: 0.40 g, 79%; elemental analysis calcd (%) for [(PhSiO₁.₅)₁₂(CuO)₆]: Cu 18.80, Si 16.62; found (in a vacuum-dried sample): Cu 18.70, Si 16.54.

Synthesis of 6

Compound 6a: Compound **1** (0.5 g, 0.33 mmol) was dissolved in a mixture of toluene (20 mL) and 1,4-dioxane (30 mL). The reaction mixture was brought to reflux and anhydrous $CuCl_2$ (0.068 g, 0.5 mmol) in methanol (10 mL) was added dropwise, along with simultaneous distillation of the solution to completely remove methanol from reaction mixture. When 10 mL of distillate was collected, water (2 mL) was added to the rest of reaction mixture, then the mixture was cooled to room temperature, and filtered into an evaporation flask. The flask was equipped with a septum and needle to allow solvents to evaporate under a slow current of nitrogen. Immediately after blue-colored crystals began to form, the flask was transferred to the fridge and stored there until the crystal fraction growth (3–4 weeks) ceased, as visually determined. A few selected monocrystals were used for the X-ray study (for details, see below). Yield: 0.11 g, 20 %; elemental analysis calcd (%) for [(PhSiO$_{1.5}$)$_{12}$(CuO)$_6$(NaCl)]: Cl 1.70, Cu 18.28, Na 1.10, Si 16.16; found (in a vacuum-dried sample): Cl 1.66, Cu 18.19, Na 1.06, Si 16.09.

Compound 6b: Compound **2** (0.5 g, 0.25 mmol) was dissolved in the mixture of toluene (20 mL) and 1,4-dioxane (30 mL). The reaction mixture was brought to reflux and anhydrous $CuCl_2$ (0.068 g, 0.5 mmol) in methanol (10 mL) was added dropwise, along with simultaneous distillation of the solution to completely remove methanol from the reaction mixture. When 10 mL of distillate was collected, water (2 mL) was added to the rest of reaction mixture, then mixture was cooled to room temperature, and filtered into an evaporation flask. The flask was equipped with a septum and needle to allow solvents to evaporate under a slow current of nitrogen. Immediately after blue-colored crystals began to form, the flask was transferred to the fridge and stored there until the crystal fraction growth (3–4 weeks) ceased, as visually determined. A few selected monocrystals were used for the X-ray study (cell parameters equaled those of the product, as described for **6a**). Yield: 0.35 g, 66 %; elemental analysis calcd (%) for [(PhSiO$_{1.5}$)$_{12}$(CuO)$_6$(NaCl)]: Cl 1.70, Cu 18.28, Na 1.10, Si 16.16; found (in a vacuum-dried sample): Cl 1.67, Cu 18.20, Na 1.07, Si 16.10.

Compound 6c: The same procedure as that described in **6b** was used for the synthesis with compound **3** was an initial reagent. Yield: 0.40 g, 75 %; elemental analysis calcd (%) for [(PhSiO$_{1.5}$)$_{12}$(CuO)$_6$(NaCl)]: Cl 1.70, Cu 18.28, Na 1.10, Si 16.16; found (in a vacuum-dried sample): Cl 1.66, Cu 18.18, Na 1.07, Si 16.09.

XRD studies

All measurements were carried out with Bruker Smart APEX II and Bruker APEX II DUO diffractometers. Collected reflections were integrated and corrected for absorption by using the SADABS program.[23] Crystal data and the parameters of refinement are shown in Table 7. The structures of **4**–**6** were solved by a direct method and refined in anisotropic approximation for most non-hydrogen atoms against F^2. The H atoms were calculated from the geometrical point of view and refined with constrained C−H and O−H bond length and displacement parameters. Most of the Ph groups and solvated molecules of dioxane, EtOH, and BuOH were disordered. The atoms of these moieties were split over two positions and then refined by using the rigid-body approximation. The value of occupation for several non-coordinated molecules was less than one, as revealed by analysis of their displacement factors. All calculations were carried out by using the SHELXTL PLUS[24] and OLEX II[25] software.

Quantum chemical calculations

Pure exchange-correlation functional PBE and two L1 lambda basis sets (relativistic and nonrelativistic) were chosen for the optimization.

Catalytic oxidation of benzene and alcohols

Catalysts **5** and **6** and the acids (cocatalysts HNO_3 or TFA) were used as stock solutions in acetonitrile. Aliquots of these solutions were added to the reaction mixtures. The reactions were typically carried out in air in thermostated Pyrex cylindrical vessels with vigorous stirring; the total volume of the reaction solution was 5 mL. (**CAUTION!** The combination of air or molecular oxygen and H_2O_2 with organic compounds at elevated temperatures may be explosive!) Samples of the reaction mixture were taken after certain time intervals, and concentrations of the products were measured by using the ^1H NMR spectroscopy method ([D$_6$]acetone was used as a component of the solvent and 1,4-dinitrobenzene as a standard; "Bruker AMX-400" instrument, 400 MHz).

Table 7. Crystal data for structures **4**–**6**.

	4	5	6
formula	C$_{92}$H$_{112}$Cu$_6$O$_{32}$Si$_{12}$	C$_{106}$H$_{118}$Cu$_6$N$_2$O$_{36}$Si$_{12}$	C$_{120}$H$_{159.17}$ClCu$_6$NaO$_{50}$Si$_{12}$
M_r	2448.2	2714.34	3178.40
T [K]	100	100	100
space group	P2$_1$/n	P2$_1$/n	C2/c
Z	2	2	4
a [Å]	17.8223(9)	18.2846(6)	35.9078(14)
b [Å]	18.7138(8)	19.0135(6)	17.6366(6)
c [Å]	18.9674(9)	18.9820(6)	28.1259(11)
α [°]	90.00	90.00	90.00
β [°]	113.152(2)	116.0450(10)	121.6620(10)
γ [°]	90.00	90.00	90.00
V [Å^3]	5816.6(5)	5929.0(3)	15160.8(10)
ρ_{calcd} [g cm^{-3}]	1.398	1.520	1.391
μ [cm^{-1}]	29.75	12.58	10.21
$F(000)$	4048	2796	6596.7
$2\theta_{max}$ [°]	56	61	61.5
reflns collected	52917	62045	204989
independent reflns	10183	18033	46597
independent reflns ($I > 2\sigma(I)$)	7918	13543	31958
parameters	457	732	1161
$R_1(I > 2\sigma(I))$	0.0987	0.0361	0.0843
wR_2	0.2294	0.1021	0.2857
GOF	1.047	1.041	1.018
residual electron density [e Å^{-3}] (ρ_{min}/ρ_{max})	2.391/−1.042	0.812/−0.872	1.894/−1.930

Acknowledgements

[1] a) R. Murugavel, A. Voigt, M. G. Walawalkar, H. W. Roesky, *Chem. Rev.* **1996**, *96*, 2205–2236; b) V. Lorenz, A. Fischer, S. Gießmann, J. W. Gilje, Y. Gun'ko, K. Jacob, F. T. Edelmann, *Coord. Chem. Rev.* **2000**, *206–207*, 321–368; c) R. W. Hanssen, R. A. Van Santen, H. C. Abbenhuis, *Eur. J. Inorg. Chem.* **2004**, *4*, 675–683; d) H. W. Roesky, G. Anantharaman, V. Chandrasekhar, V. Jancik, S. Singh, *Chem. Eur. J.* **2004**, *10*, 4106–4114; e) V. Lorenz, F. T. Edelmann in *Metallasilsesquioxanes, Vol. 53* (Eds.: A. F. H. Robert West, F. G. A. Stone), Academic Press, San Diego, **2005**, pp. 101–153; f) M. M. Levitsky, B. G. Zavin, A. N. Bilyachenko, *Russian Chemical Reviews* **2007**, *76*, 847; g) P. Jutzi, U. Schubert, *Silicon Chemistry*, Wiley-VCH, Weinheim, **2007**, pp. 372-394; h) A. J. Ward, A. F. Masters, T. Maschmeyer in *Advances in Silicon Science, Vol 3: Applications of Polyhedral Oligomeric Silsesquioxanes* (Ed.: C. Hartmann-Thompson), Springer, Dordrecht, **2011**, pp. 135–166.

[2] a) H. C. Abbenhuis, *Chem. Eur. J.* **2000**, *6*, 25–32; b) R. Duchateau, *Chem. Rev.* **2002**, *102*, 3525–3542; c) M. Levitskii, V. Smirnov, B. Zavin, A. Bilyachenko, A. Y. Rabkina, *Kinet. Catal.* **2009**, *50*, 490–507; d) E. A. Quadrelli, J.-M. Basset, *Coord. Chem. Rev.* **2010**, *254*, 707–728.

[3] a) U. Ritter, N. Winkhofer, R. Murugavel, A. Voigt, D. Stalke, H. W. Roesky, *J. Am. Chem. Soc.* **1996**, *118*, 8580–8587; b) G. Tan, Y. Yang, C. Chu, H. Zhu, H. W. Roesky, *J. Am. Chem. Soc.* **2010**, *132*, 12231–12233; c) Y. Li, J. Wang, Y. Wu, H. Zhu, P. P. Samuel, H. W. Roesky, *Dalton Trans.* **2013**, *42*, 13715–13722.

[4] a) A. N. Bilyachenko, M. S. Dronova, A. I. Yalymov, A. A. Korlyukov, L. S. Shul'pina, D. E. Arkhipov, E. S. Shubina, M. M. Levitsky, A. D. Kirilin, G. B. Shul'pin, *Eur. J. Inorg. Chem.* **2013**, *30*, 5240–5246; b) M. S. Dronova, A. N. Bilyachenko, A. I. Yalymov, Y. N. Kozlov, L. S. Shul'pina, A. A. Korlyukov, D. E. Arkhipov, M. M. Levitsky, E. S. Shubina, G. B. Shul'pin, *Dalton Trans.* **2014**, *43*, 872–882; c) M. M. Vinogradov, Y. N. Kozlov, A. N. Bilyachenko, D. S. Nesterov, L. S. Shul'pina, Y. V. Zubavichus, A. J. Pombeiro, M. M. Levitsky, A. I. Yalymov, G. B. Shul'pin, *New J. Chem.* **2015**, *39*, 187–199.

[5] a) A. Shilov, E. G. Shul'pin, *Russ. Chem. Rev.* **1990**, *59*, 853–867; b) G. Maravin, M. Avdeev, E. Bagrii, *Pet. Chem.* **2000**, *40*, 1–18; c) G. B. Shul'pin, *J. Mol. Catal. A* **2002**, *189*, 39–66; d) G. B. Shul'pin, *Mini-Rev. Org. Chem.* **2009**, *6*, 95–104; e) G. B. Shul'pin, *Org. Biomol. Chem.* **2010**, *8*, 4217–4228; f) A. M. Kirillov, G. B. Shul'pin, *Coord. Chem. Rev.* **2013**, *257*, 732–754; g) A. R. Silva, T. Mourão, J. Rocha, *Catal. Today* **2013**, *203*, 81–86; h) A. Sivaramakrishna, P. Suman, E. Veerashekhar Goud, S. Janardan, C. Sravani, T. Sandeep, K. Vijayakrishna, H. S. Clayton, *J. Coord. Chem.* **2013**, *66*, 2091–2109; i) G. B. Shul'pin, *Dalton Trans.* **2013**, *42*, 12794–12818; j) M. S. Holzwarth, B. Plietker, *ChemCatChem* **2013**, *5*, 1650–1679.

[6] a) I. Blain, M. Pierrot, M. Giorgi, M. Réglier, *Comptes Rendus de L'Académie des Sciences - Series IIC - Chemistry* **2001**, *4*, 1–10; b) F. d'Acunzo, P. Baiocco, M. Fabbrini, C. Galli, P. Gentili, *Eur. J. Org. Chem.* **2002**, *24*, 4195–4201; c) L. Que Jr., W. B. Tolman, *Angew. Chem. Int. Ed.* **2002**, *41*, 1114–1137; *Angew. Chem.* **2002**, *114*, 1160–1185; d) C. Gerdemann, C. Eicken, B. Krebs, *Acc. Chem. Res.* **2002**, *35*, 183–191; e) I. Blain, P. Slama,

M. Giorgi, T. Tron, M. Réglier, *Rev. Mol. Biotechnol.* **2002**, *90*, 95–112; f) J. M. Bollinger Jr, C. Krebs, *Curr. Opin. Chem. Biol.* **2007**, *11*, 151–158; g) R. A. Himes, K. D. Karlin, *Curr. Opin. Chem. Biol.* **2009**, *13*, 119–131; h) A. Kunishita, M. Z. Ertem, Y. Okubo, T. Tano, H. Sugimoto, K. Ohkubo, N. Fujieda, S. Fukuzumi, C. J. Cramer, S. Itoh, *Inorg. Chem.* **2012**, *51*, 9465–9480.

[7] a) J. A. R. Salvador, J. H. Clark, *Green Chem.* **2002**, *4*, 352–356; b) J. Le Bras, J. Muzart, *J. Mol. Catal. A* **2002**, *185*, 113–117; c) G. B. Shul'pin, J. Gradinaru, Y. N. Kozlov, *Org. Biomol. Chem.* **2003**, *1*, 3611–3617; d) E. A. Lewis, W. B. Tolman, *Chem. Rev.* **2004**, *104*, 1047–1076; e) T. Punniyamurthy, L. Rout, *Coord. Chem. Rev.* **2008**, *252*, 134–154; f) M. V. Kirillova, Y. N. Kozlov, L. S. Shul'pina, O. Y. Lyakin, A. M. Kirillov, E. P. Talsi, A. J. L. Pombeiro, G. B. Shul'pin, *J. Catal.* **2009**, *268*, 26–38; g) K. D. Karlin, S. Itoh, S. Rokita, *Copper–Oxygen Chemistry*, Wiley, Hoboken, NJ, **2011**; h) A. M. Kirillov, M. V. Kirillova, A. J. L. Pombeiro, *Coord. Chem. Rev.* **2012**, *256*, 2741–2759; i) T. C. O. Mac Leod, M. N. Kopylovich, M. F. C. Guedes d Silva, K. T. Mahmudov, A. J. L. Pombeiro, *Applied Catal. A: General* **2012**, *439–440*, 15–23; j) P. Nagababu, S. Maji, M. P. Kumar, P. P. Y. Chen, S. S. F. Yu, S. I. Chan, *Adv. Synth. Catal.* **2012**, *354*, 3275–3282; k) S. Kim, C. Saracini, M. A. Siegler, N. Drichko, K. D. Karlin, *Inorg. Chem.* **2012**, *51*, 12603–12605; l) P. Vanelderen, J. Vancauwenbergh, B. F. Sels, R. A. Schoonheydt, *Coord. Chem. Rev.* **2013**, *257*, 483–494; m) O. Perraud, A. B. Sorokin, J.-P. Dutasta, A. Martinez, *Chem. Commun.* **2013**, *49*, 1288–1290; n) S. E. Allen, R. R. Walvoord, R. Padilla-Salinas, M. C. Kozlowski, *Chem. Rev.* **2013**, *113*, 6234–6458; o) M. Nandia, P. Royb, *Indian J. Chem. Sect. A* **2013**, *52*, 1263–1268; p) O. V. Nesterova, E. N. Chygorin, V. N. Kokozay, V. V. Bon, I. V. Omelchenko, O. V. Shishkin, J. Titis, R. Boca, A. J. L. Pombeiro, A. Ozarowski, *Dalton Trans.* **2013**, *42*, 16909–16919.

[8] a) G. Ragagnin, B. Betzemeier, S. Quici, P. Knochel, *Tetrahedron* **2002**, *58*, 3985–3991; b) M. V. Kirillova, A. M. Kirillov, D. Mandelli, W. A. Carvalho, A. J. L. Pombeiro, G. B. Shul'pin, *J. Catal.* **2010**, *272*, 9–17; c) A. M. Kirillov, M. V. Kirillova, L. S. Shul'pina, P. J. Figiel, K. R. Gruenwald, M. F. C. Guedes da Silva, M. Haukka, A. J. L. Pombeiro, G. B. Shul'pin, *J. Mol. Catal. A* **2011**, *350*, 26–34; d) Y. Pérez, R. Ballesteros, M. Fajardo, I. Sierra, I. del Hierro, *J. Mol. Catal. A* **2012**, *352*, 45–56.

[9] a) L. Noreña-Franco, I. Hernandez-Perez, J. Aguilar-Pliego, A. Maubert-Franco, *Catal. Today* **2002**, *75*, 189–195; b) W. Buijs, P. Comba, D. Corneli, H. Pritzkow, *J. Organomet. Chem.* **2002**, *641*, 71–80; c) L. S. Shul'pina, K. Takaki, T. V. Strelkova, G. B. Shul'pin, *Pet. Chem.* **2008**, *48*, 219–222; d) A. Conde, M. Mar Diaz-Requejo, P. J. Perez, *Chem. Commun.* **2011**, *47*, 8154–8156.

[10] a) L. U. Nordstrøm, H. Vogt, R. Madsen, *J. Am. Chem. Soc.* **2008**, *130*, 17672–17673; b) C. Gunanathan, Y. Ben-David, D. Milstein, *Science* **2007**, *317*, 790–792; c) T. Naota, S.-I. Murahashi, *Synlett* **1991**, 693–694.

[11] a) T. Zweifel, J. V. Naubron, H. Grutzmacher, *Angew. Chem. Int. Ed.* **2009**, *48*, 559–563; *Angew. Chem.* **2009**, *121*, 567–571; b) K.-i. Fujita, Y. Takahashi, M. Owaki, K. Yamamoto, R. Yamaguchi, *Org. Lett.* **2004**, *6*, 2785–2788.

[12] a) X. Bantreil, N. Kanfar, N. Gehin, E. Golliard, P. Ohlmann, J. Martinez, F. Lamaty, *Tetrahedron* **2014**, *70*, 5093–5099; b) X.-F. Wu, M. Sharif, A. Pews-Davtyan, P. Langer, K. Ayub, M. Beller, *Eur. J. Org. Chem.* **2013**, 2783–2787; c) S. C. Ghosh, J. S. Y. Ngiam, A. M. Seayad, D. T. Tuan, C. W. Johannes, A. Chen, *Tetrahedron Lett.* **2013**, *54*, 4922–4925; d) S. Gaspa, A. Porcheddu, L. De Luca, *Org. Biomol. Chem.* **2013**, *11*, 3803–3807; e) X. Bantreil, C. Fleith, J. Martinez, F. Lamaty, *ChemCatChem* **2012**, *4*, 1922–1925; f) X. Bantreil, P. Navals, J. Martinez, F. Lamaty, *Eur. J. Org. Chem.* **2015**, *2*, 417–422.

[13] a) F. J. Feher, K. Rahimian, T. A. Budzichowski, J. W. Ziller, *Organometallics* **1995**, *14*, 3920–3926; b) R. Duchateau, H. C. L. Abbenhuis, R. A. van Santen, S. K. H. Thiele, M. F. H. van Tol, *Organometallics* **1998**, *17*, 5222–5224; c) H. C. L. Abbenhuis, R. A. van Santen, A. D. Burrows, M. T. Palmer, H. Kooijman, M. Lutz, A. L. Spek, *Chem. Commun.* **1998**, 2627–2628; d) V. Lorenz, A. Fischer, F. T. Edelmann, *Inorg. Chem. Commun.* **2000**, *3*, 292–295; e) V. Lorenz, A. Fischer, F. T. Edelmann, *Z. Anorg. Allg. Chem.* **2000**, *626*, 1728–1730; f) E. A. Quadrelli, J. E. Davies, B. F. G. Johnson, N. Feeder, *Chem. Commun.* **2000**, 1031–1032; g) P. L. Arnold, A. J. Blake, S. N. Hall, B. D. Ward, C. Wilson, *J. Chem. Soc. Dalton Trans.* **2001**, 488–491; h) V. Lorenz, A. Fischer, F. T. Edelmann, *J. Organomet. Chem.* **2002**, *647*, 245–249; i) V. Lorenz, S. Gießmann, Y. K. Gun'ko, A. K. Fischer, J. W. Gilje, F. T. Edelmann, *Angew. Chem. Int. Ed.* **2004**, *43*, 4603–4606; *Angew. Chem.* **2004**, *116*, 4703–4706; j) N. V. Sergienko, E. S. Trankina, V. I.

Pavlov, A. A. Zhdanov, K. A. Lyssenko, M. Y. Antipin, E. I. Akhmet"eva, *Russ. Chem. Bull.* **2004**, *53*, 351–357; k) B. G. Zavin, N. V. Sergienko, A. A. Korlyukov, V. D. Myakushev, M. Y. Antipin, *Mendeleev Commun.* **2008**, *18*, 76–77; l) N. Sergienko, N. Cherkun, A. Korlyukov, A. Sochikhin, V. Myakushev, T. Strelkova, B. Zavin, *Russ. Chem. Bull.* **2013**, *62*, 1999–2006.

[14] V. A. Igonin, O. I. Shchegolikhina, S. V. Lindeman, M. M. Levitsky, Y. T. Struchkov, A. A. Zhdanov, *J. Organomet. Chem.* **1992**, *423*, 351–360.

[15] a) G. L. Abbati, A.-L. Barra, A. Caneschi, A. Cornia, A. F. Costantino, D. Gatteschi, Y. A. Pozdniakova, O. I. Shchegolikhina, *C. R. Chim.* **2003**, *6*, 645–656; b) S. V. Lindeman, O. I. Shchegolikhina, Y. A. Molodtsova, A. A. Zhdanov, *Acta Crystallogr. Sect. C* **1997**, *53*, 305–309.

[16] a) V. A. Blatov, *IUCr CompComm Newsletter* **2006**, *7*; b) G. E. Kostakis, V. A. Blatov, D. M. Proserpio, *Dalton Trans.* **2012**, *41*, 4634–4640; c) G. E. Kostakis, S. P. Perlepes, V. A. Blatov, D. M. Proserpio, A. K. Powell, *Coord. Chem. Rev.* **2012**, *256*, 1246–1278.

[17] E. Alexandrov, V. Blatov, A. Kochetkov, D. Proserpio, *CrystEngComm* **2011**, *13*, 3947–3958.

[18] a) M. O'Keeffe, O. M. Yaghi, *Chem. Rev.* **2012**, *112*, 675–702; b) V. A. Blatov, D. M. Proserpio, *Modern Methods of Crystal Structure Prediction*, Wiley-VCH, Weinheim, **2011**, pp. 1–28; c) V. Blatov, M. O'Keeffe, D. Proserpio, *CrystEngComm* **2010**, *12*, 44–48.

[19] a) G.-C. Kuang, P. M. Guha, W. S. Brotherton, J. T. Simmons, L. A. Stankee, B. T. Nguyen, R. J. Clark, L. Zhu, *J. Am. Chem. Soc.* **2011**, *133*, 13984–14001; b) M. Du, C.-P. Li, J.-M. Wu, J.-H. Guo, G.-C. Wang, *Chem.*

Commun. **2011**, *47*, 8088–8090; c) W. Lu, D. Yuan, A. Yakovenko, H.-C. Zhou, *Chem. Commun.* **2011**, *47*, 4968–4970; d) Z. Hulvey, J. D. Furman, S. A. Turner, M. Tang, A. K. Cheetham, *Cryst. Growth Des.* **2010**, *10*, 2041–2043; e) P. Amo-Ochoa, L. Welte, R. González-Prieto, P. J. S. Miguel, C. J. Gómez-García, E. Mateo-Martí, S. Delgado, J. Gómez-Herrero, F. Zamora, *Chem. Commun.* **2010**, *46*, 3262–3264.

[20] F. Schax, E. Bill, C. Herwig, C. Limberg, *Angew. Chem. Int. Ed.* **2014**, *53*, 12741–12745.

[21] a) G. B. Shul'pin, D. Attanasio, L. Suber, *Russ. Chem. Bull.* **1993**, *42*, 55–59; b) G. Shul'pin, A. Druzhinina, G. Nizova, *Russ. Chem. Bull.* **1993**, *42*, 1326–1329; c) G. B. Shul'pin, Y. Ishii, S. Sakaguchi, T. Iwahama, *Russ. Chem. Bull.* **1999**, *48*, 887–890; d) M. H. de La Cruz, Y. N. Kozlov, E. R. Lachter, G. B. Shul'pin, *New J. Chem.* **2003**, *27*, 634–638.

[22] A. E. Shilov, G. B. Shul'pin, *Activation and Catalytic Reactions of Saturated Hydrocarbons in the Presence of Metal Complexes*, Kluwer Academic Publishers, Dordrecht/Boston/London, 2000, p. 548.

[23] R. H. Blessing, *Acta Crystallogr. Sect. A* **1995**, *51*, 33–38.

[24] G. M. Sheldrick, *Acta Crystallogr. Sect. A* **2008**, *64*, 112–122.

[25] O. V. Dolomanov, L. J. Bourhis, R. J. Gildea, J. A. Howard, H. Puschmann, *J. Appl. Crystallogr.* **2009**, *42*, 339–341.